ACTA ODONTOLOGICA SCANDINAVICA
2019, VOL. 77, NO. 1, 49–54
https://doi.org/10.1080/00016357.2018.1499959

Taylor & Francis
Taylor & Francis Group

ORIGINAL ARTICLE

Dental magnetic resonance imaging for periodontal indication – a new approach of imaging residual periodontal bone support

Maurice Ruetters[a], Alexander Juerchott[b], Nihad El Sayed[a], Sabine Heiland[b], Martin Bendszus[b] and Ti-Sun Kim[a]

[a]Section of Periodontology, Clinic for Conservative Dentistry, University Hospital Heidelberg, Heidelberg, Germany; [b]Division of Neuroradiology, Department of Neurology, University Hospital Heidelberg, Heidelberg, Germany

ABSTRACT

Objective: The standard imaging techniques used in dentistry consist of two-dimensional radiographic techniques like intraoral periapical (PA) radiographs, bitewings or extraoral panoramic X-rays. Three-dimensional methods, such as cone beam computed tomography (CBCT), are not standard procedures. In several fields of dentistry, such as oral surgery or implantology, dental magnetic resonance imaging (DMRI), a technique without radiation exposure, has already been introduced as a new promising diagnostic tool. The aim of this study was to compare the agreement of DMRI and PA radiographs in measuring residual periodontal bone support.

Material and methods: In this study, the residual periodontal bone support of 21 teeth was investigated and compared with DMRI and PA radiographs by two independent raters. Intra-class correlation coefficients (ICCs) were calculated using the software R to identify the intra-rater and inter-rater agreement of the two modalities. Bland–Altman plots were created to directly compare the two methods.

Results: Overall, all calculated ICC values showed an excellent intra-rater and inter-rater agreement (>0.9) for DMRI, as well as PA radiographs. Bland–Altman analysis also showed a strong agreement between both diagnostic methods in this study.

Conclusions: In conclusion, there was a strong agreement between DMRI and PA. Thus, DMRI proved to be a comparable method to PA radiographs for evaluating the proportion of residual periodontal bone support.

ARTICLE HISTORY
Received 7 March 2018
Revised 7 June 2018
Accepted 24 June 2018

KEYWORDS
Magnetic resonance imaging; X-rays; periodontal disease; dental digital radiography; periodontal attachment loss; diagnostic imaging

Introduction

The standard imaging techniques used in dentistry consist of two-dimensional radiographic techniques like intraoral periapical (PA) radiographs, bitewings or extraoral panoramic X-rays. Three-dimensional methods, such as cone beam computed tomography (CBCT), are not standard procedures because of the high dose of radiation involved. Imaging without any radiation is the safest method for the patient to avoid exposure to radiation and to fulfill the as low as diagnostically achievable (ALADA) principle.

In several fields of dentistry, such as oral surgery or implantology, magnetic resonance imaging (MRI), a technique without X-ray exposure, has already been introduced as a new promising diagnostic tool. For example, MRI can display the alveolar mandibular nerve very well and may also reduce the rate of iatrogenic injuries in surgical procedures [1]. Some disorders can be detected at an early stage [2,3]. So far, there are only a few studies investigating the imaging of periodontal structures in dental magnetic resonance imaging (DMRI) [4–6]. It has been shown that PA lesions can be illustrated with DMRI, as well as vital pulps and the periodontal ligament [4–7]. Moreover, it may help detect periodontal lesions earlier than radiographs, as DMRI can visualize soft tissue and inflamed tissue with a high sensitivity. Kito et al. compared DMRI with PET-CT and showed a correlation concerning inflammation signs in the periodontium [8]. Schara et al. showed an association between clinical parameters and relaxation times of gingival tissues *in vitro* DMRI. They also demonstrated a decrease of contrast signal intensity with the improvement of clinical parameters *in vivo* [9]. The authors have found no data on the precision and agreement of DMRI imaging of periodontal lesions in comparison with established radiographic methods like intraoral PA radiographs in the current literature.

The aim of this proof of principle study was to compare the agreement of DMRI and PA radiographs in measuring residual periodontal bone support.

Materials and methods

Study population

There were five patients included in this feasibility study (two females and three males, mean age 47.8 years, range 34–68 years.). Patients had to be diagnosed as periodontally

CONTACT Maurice Ruetters maurice.ruetters@med.uni-heidelberg.de Section of Periodontology, Clinic for Conservative Dentistry, University Hospital Heidelberg, Im Neuenheimer Feld 400, Heidelberg 69115, Germany

Supplemental data for this article can be accessed here.

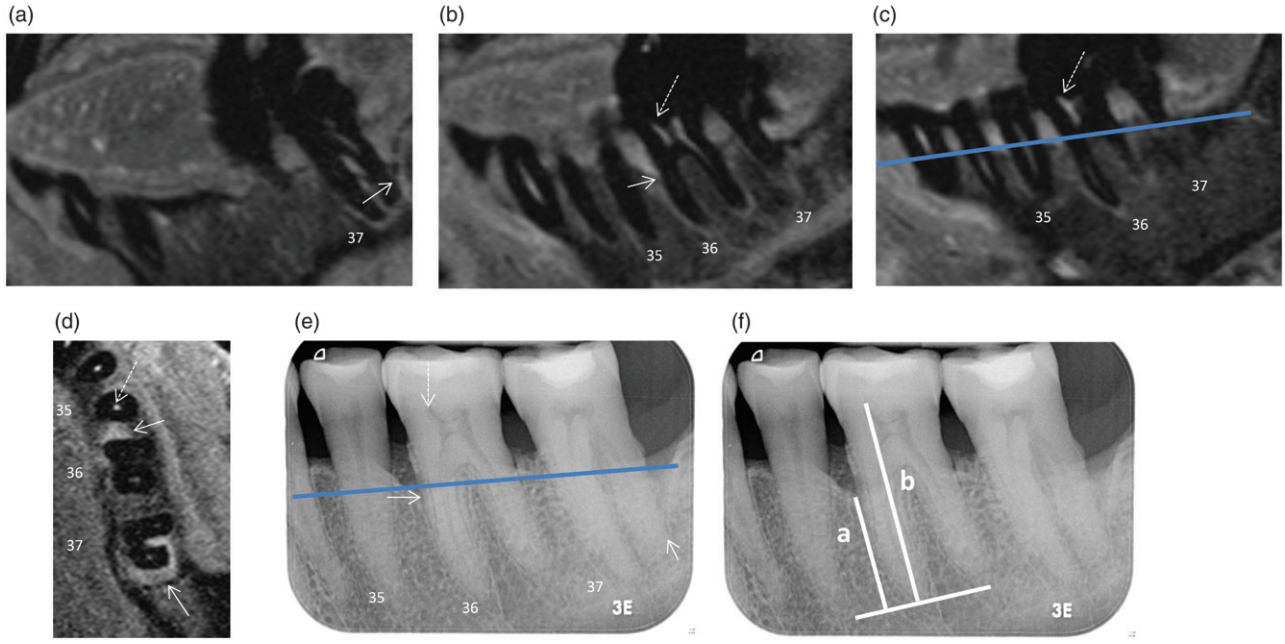

Figure 1. T1-DMR images of the left jaw parasagittal with contrast agent (Dotarem). (a–c) Parasagittal images scrolled from oral to buccal. White arrows: bottom of the distal bony defect (least residual periodontal bone support) of teeth 36 and 37, white interrupted arrows: pulp of teeth 36 and 37. The deepest point of the least mesial residual periodontal bone support of tooth 36 can be seen in (b) and the least distal residual periodontal bone support of tooth 37 can be seen in (a). (d) According axial images at the level of the blue line. Interestingly, one can see that the mesial defect of at tooth 36 is located more to the lingual aspect of root, whereas the distal defect of tooth 37 involves even the furcation area. (e) According periapical radiograph (f) Measurement in PA-radiographs: *a*: distance from the apex to the bottom of the bony defect, *b*: distance from the apex to the top of the pulp horn, $q = a/b$. The same measurements were performed in the MR images (Figure 2).

affected according to the classification of Armitage [10]. For that reason, a complete periodontal examination was performed including clinical attachment loss and clinical pocket depth at six sites per tooth with a periodontal probe (PCPUNC 15) at the University Hospital Heidelberg in the Section of Periodontology of the Department of Restorative Dentistry. Tooth vitality of included teeth was considered as an inclusion criterion for this study. Endodontic treatment and extensive restorations close to the pulp were considered as tooth-related exclusion criteria to avoid any artifacts in the pictures and to be able to detect the pulp in both imaging methods as reference [11]. Twenty-one teeth met these criteria and were included in the study. The patients had to be free of any conditions that do not allow a DMRI to be taken, for example, pacemakers, insulin pumps, metallic implants and claustrophobia.

All patients gave informed consent to participate in the study. The study protocol was approved by the ethics committee at the University Hospital Heidelberg (file number: S-452/2010).

Radiographic and DMRI examination

One DMRI was taken of each patient at the Clinic of Neuroradiology of the University Hospital Heidelberg with a 3T DMRI system (Magnetom Trio; Siemens AG, Erlangen, Germany). A dedicated 16-channel-surface coil (NORAS MRI products, Höchberg, Germany) was used. A scanning protocol optimized for high resolution imaging of teeth and periodontium was applied including T2 and T1 weighted Turbo Spin Echo Sequences. Patients received the contrast agent Dotarem® (Guerbet, BP 57400, 95943 Roissy CdG Cedex, France), intravenously. All measurements of periodontal defects were performed on a contrast-enhanced, fat-saturated T1 weighted sequence with a repetition time (TR) of 580 ms, an echo time (TE) of 11 ms, a slice thickness of 1mm, 0.469×0.469 mm pixel spacing and a field of view of 120 mm × 120 mm. The overall acquisition time was 20 minutes. Each patient additionally received intraoral PA radiographs of the included teeth if clinically indicated as the diagnostic reference standard (Sirona Heliodent DS, 60kV 7mA, phosphor stimulable plate, Dürr Dental, Software DuerrScan 1.0). The DMRI and corresponding PAs had to be taken within 1 month.

DMRI and the PA radiographs were analyzed by two raters, one dentist and one radiologist, each of them with at least 4 years of clinical experience. All PA radiographs and DMRIs were measured twice. The investigators were blinded to each other and blinded between the two methods. Quantitative analysis was performed on a SIEMENS Syngo Workstation (Syngo MMWP VE31A, syngVE32B, Erlangen, Germany) by the two investigators.

The examination method is described in Figures 1 and 2. In PA radiographs the distance between the apex of the root and the deepest point of the bony defect of each tooth was measured mesially and distally (= *a*) and compared with the distance between the apex of the root and the corresponding pulp-horn of the tooth (= *b*). The deepest point of the bony defect was defined as the most coronal point where periodontal ligament space showed a continuous width [12]. The pulp horn was determined as a relevant reference mark by consensus amongst all authors because it provides the

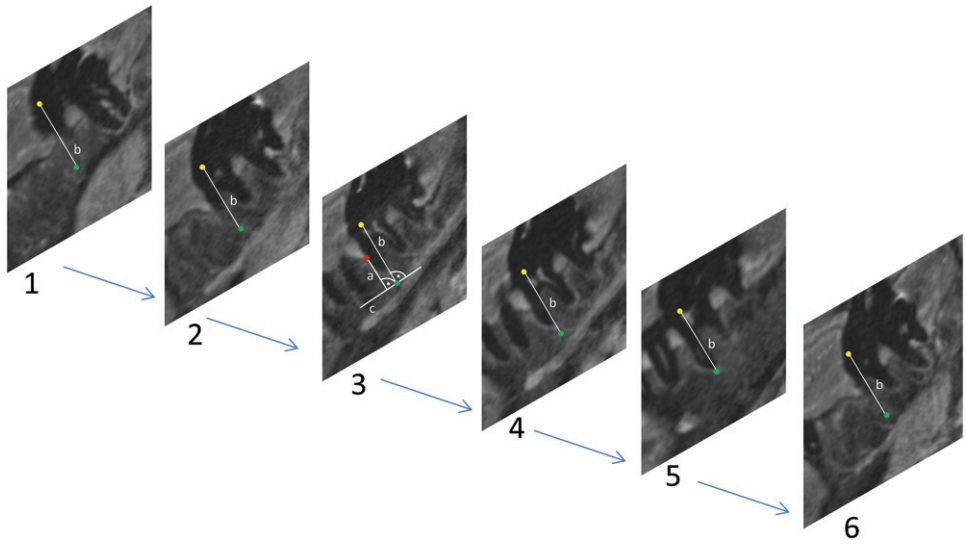

Figure 2. Illustration of measurement method in DMRI for the measurements of the residual bone height at the mesial root of tooth 36. (1–6) DMRI images of tooth 36 scrolled from oral to buccal. Yellow dot: location of the mesial pulp horn (highest location in image 5), green dot: location of the apex of the mesial root (image 5), red dot: deepest point of the mesial bony defect (image 3). Accordingly, a ratio q (= a/b) was calculated and compared.

Table 1. ICC values to investigate the inter- and intra-rater agreement.

ICC r1 DMRI1 vs DMRI2 (RBS)	0.992
ICC r1 PA1 vs PA2 (RBS)	0.953
ICC r2 DMRI1 vs DMRI2 (RBS)	0.993
ICC r2 PA1 vs PA2 (RBS)	0.995
ICC r1 DMRI vs r2 DMRI (RBS)	0.977
ICC r1 PA vs r2 PA (RBS)	0.969

ICC: intra-class correlation coefficient; DMRI1: first measurements of DMRI; DMRI2: second measurements of DMRI; PA1: first measurements of PA radiographs; PA2: second measurements of PA radiographs; RBS: residual bone support, r: rater.

advantage to be reliably detectable in PA radiographs as well as in DMRI. Other alternatives such as the Cemento-Enamel-Junction (CEJ) were considered less useful because they cannot be identified in DMRI. The absolute measurements could not be used for a comparative study, due to the different angulations of the two methods PA radiographs and DMRI. Accordingly, a ratio q (= a/b) was calculated and compared. The same anatomic landmarks were pointed out in DMRI and the same distances were measured by scrolling through the associated images in parasagittal and coronal sections to be able to calculate the ratio q. The method of identifying the landmarks is described in Figure 2. DMRI images were scrolled through from oral to buccal. The location of the highest detectable pulp horn was marked in the according picture. This point was transferred in all other pictures by software. Afterwards the location of the apex of the root was pointed out in the according picture and transferred in all others pictures by software. The distance between these two points represents distance b. Then the deepest point of the bony defect was marked. A line was drawn perpendicular to distance b from the apex of the tooth named line c. Then another line was drawn perpendicular to c from the deepest point of the bony defect. The distance between line c and the deepest point of the bony defect represents distance a. Accordingly, a ratio q (= a/b) was calculated and compared (Figure 2). The measurements of molars and premolars based on DMRI data were performed in the parasagittal sections and the measurements of anterior teeth in the coronal sections.

The ratio q, as a targeted parameter, was used to compare these two methods concerning measurements of residual bone height. Bland–Altman plots were created to compare the two methods for statistical analysis. The intra-class correlation coefficient (ICC) was calculated to identify both the inter-rater and the intra-rater agreement by using the software *R* in combination with the packages 'irr', 'lpSolve' and 'xtable' [13–16]. Consequently, the absolute measurements of the residual bone height were used as a targeted parameter.

Results

While taking the PA radiographs and the DMRIs with Dotarem, no adverse reactions occurred and no patient showed discomfort.

In total, 21 teeth were measured at 41 sites twice, at 5 DMRIs and 10 corresponding PA radiographs. Six of the teeth were anterior teeth, 11 premolars and 4 molars. Ten teeth were located in the lower jaw and 11n teeth in the upper jaw. The mean clinical probing depth was 4.5 ± 2.8 mm and the mean clinical attachment level was 5.7 ± 2.7 mm.

First, the intra-rater agreement of the two methods DMRI and PA radiographs were determined by the ICC of the measurements of the residual bone height. High ICC-values of 0.992 (rater 1) and 0.993 (rater 2) for DMRI and 0.953 (rater 1) and 0.995 (rater 2) for PA radiographs were observed. Analyzing the inter-rater agreement ICC values of 0.977 (DMRI) and 0.969 (PA radiographs) were calculated (Table 1). Actual measurements have been added as a supplementary file.

Two Bland–Altman plots were created by using the ratio q to compare the two methods. Three lines are implemented within each plot to achieve an easier interpretation. The dashed lines show the mean value ± 1.96 standard deviation, meaning that 95% of the values are in between these lines.

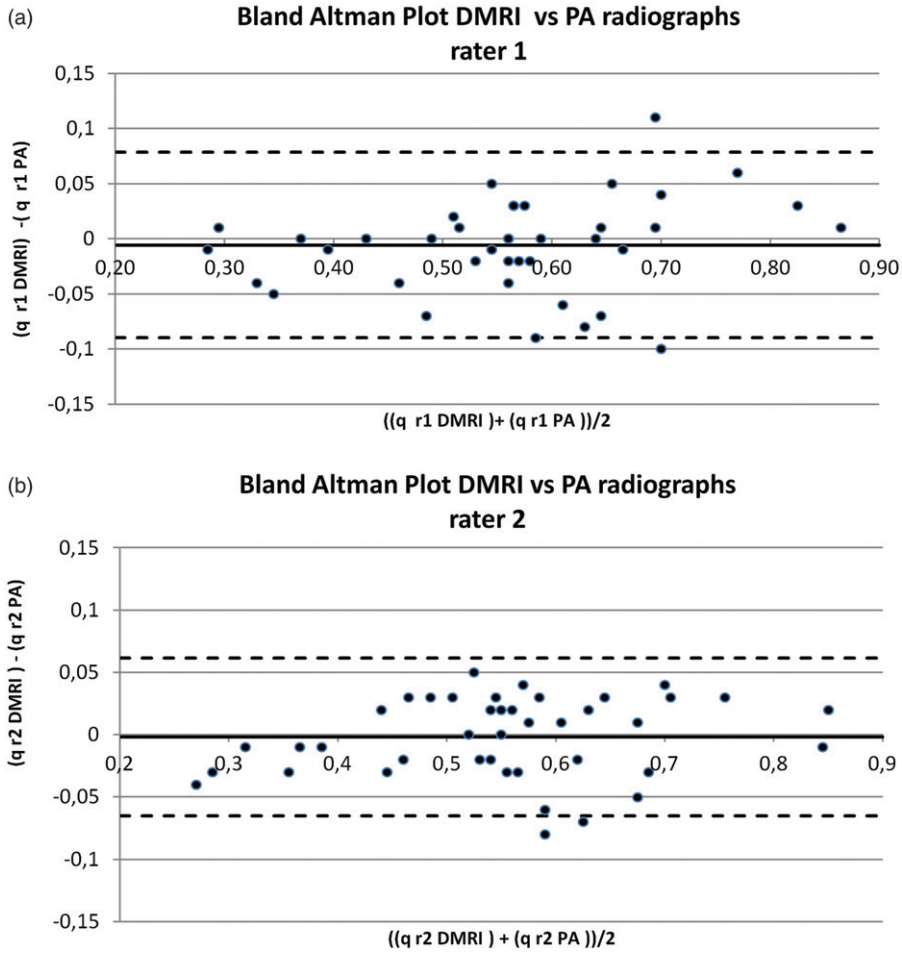

Figure 3. Bland–Altman plots. (a) Bland–Altman Plot rater 1: The mean difference is –0.0056 (solid line). 95% of values are in between 0.07 (upper dashed line) and –0.09 (lower dashed line). (b) Bland–Altman plot rater 2: The mean difference is –0.0019 (solid line). 95% of values are in between 0.06 (upper dashed line) and –0.07 (lower dashed line).

The solid line indicates the mean of differences. Both raters' results indicate that there is a strong correlation between these two methods. Rater 1 has a mean of differences of ratio *q* of –0.0056 ± 0.043; whereas, rater 2 has a mean of differences of ratio *q* of –0.0019 ± 0.032. 95% of the differences between the methods were in the range of 0.07 and –0.09 for rater 1 and 0.06 and –0.07 for rater 2 (Figure 3). The ICC of the measurements of the distance b were calculated with the goal of excluding significant errors of *q*. Comparing the measurements of rater 1 versus those of rater 2 resulted in ICC values of 0.931 (DMRI) and 0.904 (PA radiographs), respectively

Discussion

The findings of the present study indicate excellent agreement of DMRI and PA radiographs when measuring residual periodontal bone support. The high ICC-values of more than 0.9 indicate high inter-rater and intra-rater agreement of both modalities. Thus, DMRI and PA radiographs that is the reference method in our study, showed high levels of reliability and reproducibility.

Two Bland–Altman plots allow for the direct comparison of the two methods by using the ratio *q*. Only minor differences of *q* (mean difference –0.0056 ± 0.043 (rater 1) and –0.00196 ± 0.032 (rater 2)) and a small range of 95% of measurements (0.07 and –0.09 rater 1 and 0.06 and –0.07 rater 2) strongly concur the agreement between the two measurement methods. In addition, neither PA radiographs nor DMRI seem to over- or underestimate residual bone support independent of lower values of *q*, indicating little residual bone height, or higher values of *q*, indicating more residual bone height shown by the mean differences around the reference point, 0.

A few limitations of the present study should be mentioned:

Firstly, there were differences in angulation between the two methods, prohibiting a direct comparison of absolute values. However, these differences were accounted for by using the ratio *q*.

PA radiographing, not clinical measurements, was the reference technique in this study because none of the routine clinical measurements, PD or CAL, can be transferred into the DMRI datasets used in this study. The anatomic landmarks margin of the gingiva (PD) or CEJ (CAL) cannot be identified on DMRI due to artifacts by the tongue. PA radiographs have previously been shown not to differ statistically in terms of linear measurements of residual periodontal bone support compared to intraoperative measurements. [17] Thus, PA radiographing was chosen as a reference. The measurements applied in our study represented

measurements of soft tissue (distance *a*) as well as of hard tissue (distance *b*). They demonstrate the accuracy of DMRI as a matter of principle concerning periodontal structures. Three-dimensional visualization of a periodontal defect, such as a furcation defect or a vertical defect, can be of prognostic value for the clinician. In the future, the morphology of periodontal defects may be illustrated and calculated by DMRI similar to CBCT but without radiation. This could be enabled using novel DMRI techniques that allow for three-dimensional imaging of periodontal tissue [18–21]. Secondly, the resolution of the DMRI sequence used in this study may be questioned. However, the DMRI sequence used in this study had an in-plane resolution of 0.469×0.469 mm which was one of the highest achievable resolutions available at the time of this study. Although DMRI cannot yet equal the resolution of PA radiographs, the achieved resolution is within the clinical tolerance level of 0.5 mm. Future technological developments may improve resolution capabilities [22,23], and subpixel algorithms enable a more precise imaging than the actual resolution would allow [24]. Thirdly, in practice, not all patients are suitable to receive DMRI, but most of them can receive a PA; for example, patients with cardiac pacemakers, insulin pumps, metallic implants and claustrophobia. Furthermore, there are materials used in dentistry that cause artifacts in DMRI, such as stainless steel orthodontic appliances and CoCr alloys [11]. A relative disadvantage of this study may be the use of contrast agent for DMRI. Although evidence shows that the use of the contrast agent Dotarem® is safe [25,26], it takes more time to apply the agent. Adverse reactions may occur and, moreover, patients treated with the contrast agent have a tendency to feel discomfort compared with patients on whom this agent was not used. In this study population, none of the patients showed adverse reactions after the use of Dotarem®. Fourth, DMRI devices are currently relatively expensive and not as widely accessible to dentists compared with X-ray methods. MRI scanners are operated by qualified radiologists and not by dentists. Therefore, more manpower is required to conduct a DMRI. Acquisition time is much longer for DMRI compared with a PA. Taking a PA represents a fast imaging method, which can be conducted by a dentist. However, DMRI is a relatively new technique and technical improvements may result in faster acquisition times, and more affordable equipment, suitable for use in a dental office. Similarly to CBCT, which was very expensive when first introduced, but is now quite affordable.

Despite all these limitations, one must consider that DMRI represents an imaging technique without any ionizing radiation. This is a major advantage compared to contemporary patient imaging techniques. Although the impact of dental radiology on the health of the oral cavity and its surrounding structures is not well known, radiation should be avoided as much as possible. Several technical improvements such as digital charge-coupled device sensors and the use of rectangular collimation have already reduced the amount of necessary radiation, although it cannot be avoided altogether [27,28].

Within the limitations of the study, there was a strong agreement between DMRI and PA, and DMRI proved to be a comparable method to PA radiographs for evaluating the proportion of residual periodontal bone support. Further studies are required before implementing this new approach to the clinical routine in dentistry.

Acknowledgements

The authors kindly thank NORAS MRI products GmbH (Höchberg, Germany) for providing the 16-channel multipurpose coil.

Disclosure statement

No potential conflict of interest was reported by the authors.

References

[1] Kress B, Gottschalk A, Anders L, et al. Topography of the inferior alveolar nerve in relation to cystic processes of the mandible in dental MRI. Rofo. 2003;175:67–69.

[2] Sedlacik J, Kutzner D, Khokale A, et al. Optimized 14 + 1 receive coil array and position system for 3D high-resolution MRI of dental and maxillomandibular structures. Dentomaxillofac Radiol. 2016;45:20150177.

[3] Fujii H, Fujita A, Yang A, et al. Visualization of the peripheral branches of the mandibular division of the trigeminal nerve on 3D Double-Echo Steady-State with Water Excitation Sequence. Am J Neuroradiol. 2015;36:1333–1337.

[4] Gaudino C, Cosgarea R, Heiland S, et al. MR-imaging of teeth and periodontal apparatus: an experimental study comparing high-resolution MRI with MDCT and CBCT. Eur Radiol. 2011;21:2575–2583.

[5] Prager M, Heiland S, Gareis D, et al. Dental MRI using a dedicated RF-coil at 3 Tesla. J Craniomaxillofac Surg. 2015;43:2175–2182.

[6] Gradl J, Horeth M, Pfefferle T, et al. Application of a dedicated surface coil in dental MRI provides superior image quality in comparison with a standard coil. Clin Neuroradiol. 2017;27:371–378.

[7] Geibel MA, Schreiber ES, Bracher AK, et al. Assessment of apical periodontitis by MRI: a feasibility study. Fortschr Röntgenstr. 2015;187:269–275.

[8] Kito S, Koga H, Kodama M, et al. Reflection of (1)(8)F-FDG accumulation in the evaluation of the extent of periapical or periodontal inflammation. Oral Surg Oral Med Oral Pathol Oral Radiol. 2012;114:e62–e69.

[9] Schara R, Sersa I, Skaleric U. T1 relaxation time and magnetic resonance imaging of inflamed gingival tissue. Dento Maxillo Facial Radiology. 2009;38:216–223.

[10] Armitage GC. Development of a classification system for periodontal diseases and conditions. Ann Periodontol. 1999;4:1–6.

[11] Tymofiyeva O, Vaegler S, Rottner K, et al. Influence of dental materials on dental MRI. Dentomaxillofac Radiol. 2013;42:20120271.

[12] Eickholz P, Horr T, Klein F, et al. Radiographic parameters for prognosis of periodontal healing of infrabony defects: two different definitions of defect depth. J Periodontol. 2004;75:399–407.

[13] Team RC. R: a language and environment for statistical computing: R Foundation for Statistical Computing, Vienna, Austria; 2013; [2015 Oct 06]. Available from: http://www.R-project.org/

[14] Matthias Gamer JL, Ian Fellows Puspendra Singh. Irr: various Coefficients of Interrater Reliability and Agreement. R package version 0.84. 2012; [2015 Oct 06]. Available from: http://CRAN.R-project.org/package=irr

[15] Dahl DB. xtable: export tables to LaTeX or HTML. R package version 1.7-1. 2013; [2015 Oct 06]. Available from: http://CRAN.R-project.org/package=xtable

[16] Berkelaar M. lpSolve: Interface to Lp_solve v. 5.5 to solve linear/integer programs. R package version 5.6.7. 2013; [2015 Oct 06]. Available from: http://CRAN.R-project.org/package=lpSolve
[17] Kim TS, Benn DK, Eickholz P. Accuracy of computer-assisted radiographic measurement of interproximal bone loss in vertical bone defects. Oral Surg Oral Med Oral Pathol Oral Radiol Endod. 2002;94:379–387.
[18] Dannewitz B, Krieger JK, Husing J, et al. Loss of molars in periodontally treated patients: a retrospective analysis five years or more after active periodontal treatment. J Clin Periodontol. 2006;33:53–61.
[19] Cortellini P, Tonetti MS. Clinical concepts for regenerative therapy in intrabony defects. Periodontol 2000. 2015;68:282–307.
[20] Heil A, Schwindling FS, Jelinek C, et al. Determination of the palatal masticatory mucosa thickness by dental MRI: a prospective study analysing age and gender effects. Dentomaxillofac Radiol. 2018;47:20170282.
[21] Hilgenfeld T, Kastel T, Heil A, et al. High-resolution dental magnetic resonance imaging for planning palatal graft surgery-a clinical pilot study. J Clin Periodontol. 2018;45:462–470.
[22] Zoroofi RA, Sato Y, Tamura S, et al. An improved method for MRI artifact correction due to translational motion in the imaging plane. IEEE Trans Med Imaging 1995;14:471–479.
[23] Oyre S, Ringgaard S, Kozerke S, et al. Quantitation of circumferential subpixel vessel wall position and wall shear stress by multiple sectored three-dimensional paraboloid modeling of velocity encoded cine MR. Magn Reson Med. 1998;40:645–655.
[24] Carmi E, Liu S, Alon N, et al. Resolution enhancement in MRI. Magn Reson Imaging. 2006;24:133–154.
[25] Ishiguchi T, Takahashi S. Safety of gadoterate meglumine (Gd-DOTA) as a contrast agent for magnetic resonance imaging: results of a post-marketing surveillance study in Japan. Drugs R D. 2010;10:133–145.
[26] de Kerviler E, Maravilla K, Meder JF, et al. Adverse reactions to gadoterate meglumine: review of over 25 years of clinical use and more than 50 million doses. Invest Radiol. 2016;51:544.
[27] Underhill TE, Kimura K, Chilvarquer I, et al. Radiobiologic risk estimation from dental radiology. Part II. Cancer incidence and fatality. Oral Surg Oral Med Oral Pathol. 1988;66:261–267.
[28] Anissi HD, Geibel MA. Intraoral radiology in general dental practices – a comparison of digital and film-based X-ray systems with regard to radiation protection and dose reduction. Fortschr Röntgenstr. 2014;186:762–767.